

Analyzing nonlinear mechanical-thermal buckling of imperfect micro-scale beam made of graded graphene reinforced composites

Basima Salman Khalaf, Raad M. Fenjan and Nadhim M. Faleh*

Al-Mustansiriyah University, Engineering Collage P.O. Box 46049, Bab-Muadum, Baghdad 10001, Iraq

(Received August 19, 2019, Revised September 27, 2019, Accepted October 20, 2019)

Abstract. This research is devoted to analyzing mechanical-thermal post-buckling behavior of a micro-size beam reinforced with graphene platelets (GPLs) based on geometric imperfection effects. Graphene platelets have three types of dispersion within the structure including uniform-type, linear-type and nonlinear-type. The micro-size beam is considered to be perfect (ideal) or imperfect. Buckling mode shape of the micro-size beam has been assumed as geometric imperfection. Modified couple stress theory has been used for describing scale-dependent character of the beam having micro dimension. Via an analytical procedure, post-buckling path of the micro-size beam has been derived. It will be demonstrated that nonlinear buckling characteristics of the micro-size beam are dependent on geometric imperfection amplitude, thermal loading, graphene distribution and couple stress effects.

Keywords: nonlinear buckling; graphene platelets; geometric imperfection; thermal loading; modified couple stress theory

1. Introduction

In recent decades, several carbon based structures containing carbon nanotube or carbon fiber have been widely utilized in composites for enhancing their mechanics and thermal specifications (Yazid *et al.* 2018, Mokhtar *et al.* 2018). A 273% enhancement of elastic modulus is obtained by Ahankari and Kar (2010) for carbon reinforced composites in comparison to conventional composites. Likewise, Gojny *et al.* (2004) mentioned that structural stiffness of carbon based composites may be enhanced with incorporation of carbon nanotube within material. Impacts of configuration and scale of carbon nanotubes on rigidity growth of material composites having metallic matrices are studied by Esawi *et al.* (2011). Because of possessing above mentioned properties, beam and plate structures having carbon based fillers are researched to understand their static or dynamical status, Fantuzzi *et al.* 2017, Civalek 2017, Ebrahimi and Habibi 2017, 2018, Ebrahimi and Farazmandnia 2017, Aragh 2017, Moradi-Dastjerdi and Malek-Mohammadi 2017). There are also some investigations on composite or functionally graded materials and interested readers are refaced to new investigations on materials (Singhal *et al.* 2018a, b, Singh *et al.* 2018, Nirwal *et al.* 2019, Sahu *et al.* 2018, Chaudhary *et al.* 2017, 2019a, b, Ahmed *et al.* 2019).

*Corresponding author, Professor, E-mail: dr.nadhim@uomustansiriyah.edu.iq

Furthermore, the graphene based composite material has been recently gained enormous attentions because of having easy producing procedure and high rigidity growth. Nieto *et al.* (2017) presented a review paper based on several graphene based composite material possessing ceramic or metallic matrices. The multi-scale study of mechanical attributes for graphene based composite material has been provided by Lin *et al.* (2018) utilizing finite elements approach. Wang *et al.* (2011) researched thermal attributes of graphene based composite materials.

Recently, many papers are published for investigating mechanical attributes of graphene based composite structures. Kitipornchai *et al.* (2017) studied stability as well as vibrational properties of porosity-dependent beams containing graphene based composites. Furthermore, Feng *et al.* (2017) researched large amplitude vibrations of ideal Timoshenko beams with non-uniformly diffused graphene based composites. Investigations on deflections of trapezoidal plate structures reinforced with functional gradation of graphene composites have been carried out by Zhao *et al.* (2017). Barati and Zenkour (2018a) researched vibrational attributes of graphene based shells based on Galerkin's approach. Finite elements approach is used by Reddy *et al.* (2018) to explore vibrational attributes of a laminated graphene based plate. Geometrically nonlinear vibrational attributes of scale-dependent beams made of graphene based composites are researched by Sahmani and Aghdam (2017).

Scale-dependent beam structures contains various mechanical attributes different from macro sized beam structures because of atomic interactions at micro dimensions (Ebrahimi *et al.* 2017, Bouafia *et al.* 2017, Mouffoki *et al.* 2017, Barati 2017, Semmah *et al.* 2014). At micron scales, two particles apply couple stresses to each other and experience micro rotation. Modified couple stress theory introducing one scale coefficient is one of familiar theories which is able to consider the micro rotation effects (Park and Gao 2006, Ebrahimi and Barati 2018, Fenjan *et al.* 2019, Barati and Zenkour 2018b, Singhal *et al.* 2019). Accordingly, this theory is suitable for mathematical description of micro-size structures and in particular case carbon based micobeams. Vibration properties of a carbon based microbeam in contact with elastic foundation have been studied by Shenan *et al.* (2018). Dynamic response of a microbeam made of carbon based composites subjected to harmonic loads is analyzed by Rostami *et al.* (2018) taking into account couple stress effect. Furthermore, incorporating viscoelastic influences the vibrational properties of carbon composite micro-size beam have been studied by Mohammadimehr *et al.* (2017). Also, Allahkarami and Nikkhah-Bahrami (2018) analyzed couple stress based vibration behaviors of carbon composite micro-size beams with curvature. Above published papers on microbeams constructed from carbon nanotube based composites neglected geometric imperfection influences. Several factors such as errors in production or surrounding medium may result in geometrical imperfection of the beam structures (Wu *et al.* 2016, Barati and Zenkour 2018c, Chaudhary *et al.* 2019a-c).

This paper is devoted to analyzing mechanical-thermal post-buckling behavior of a micro-size beam reinforced with graphene platelets (GPLs) based on geometric imperfection effects. Graphene platelets have three types of dispersion within the structure including uniform-type, linear-type and nonlinear-type. The micro-size beam is considered to be perfect (ideal) or imperfect. Buckling mode shape of the micro-size beam has been assumed as geometric imperfection. Modified couple stress theory has been used for describing scale-dependent character of the beam having micro dimension. Via an analytical procedure, post-buckling path of the micro-size beam has been derived. It will be demonstrated that nonlinear buckling characteristics of the micro-size beam are dependent on geometric imperfection amplitude, thermal loading, graphene distribution and couple stress effects.

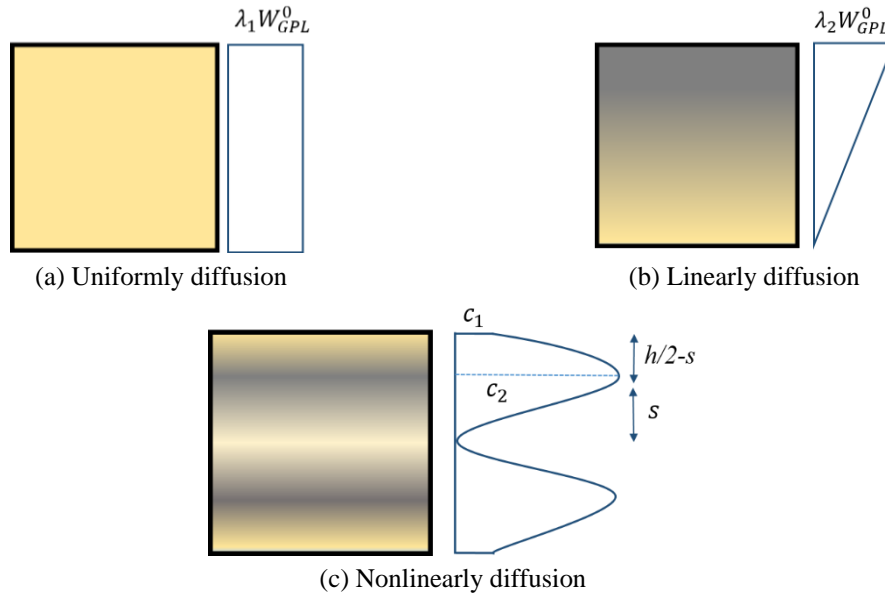


Fig. 1 Graphene diffusions in material structure

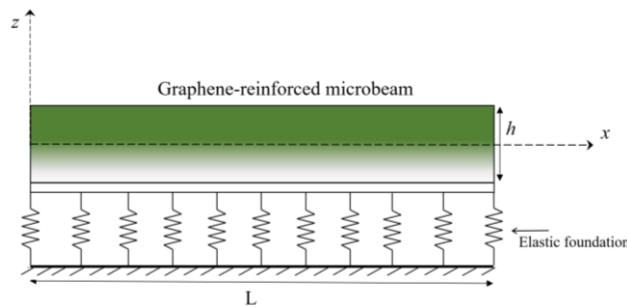


Fig. 2 Continuously graded graphene-reinforced microbeam

2. Graphene based composites

According to Fig. 1, it is assumed that graphene platelets have three types of dispersion within the structure including uniform-type, linear-type and nonlinear-type. According to Fig. 2, a graphene reinforced composite micro-scale beam is illustrated. Micro-mechanic theory of such composite materials (Barati and Zenkour 2018a) introduces the below relationship between graphene platelets weight fraction (W_{GPL}) and their volume fraction (V_{GPL}) by

$$V_{GPL} = \frac{W_{GPL}}{W_{GPL} + \frac{\rho_{GPL}}{\rho_M} - \frac{\rho_{GPL}}{\rho_M} W_{GPL}} \quad (1)$$

where ρ_{GPL} and ρ_M define the mass densities of graphene and polymeric matrices, respectively. Next, the elastic modulus of a graphene based composite might be represented based upon matrix

elastic modulus (E_M) by (Barati and Zenkour 2018a)

$$E_1 = \frac{3}{8} \left(\frac{1 + \xi_L^{GPL} \eta_L^{GPL} V_{GPL}}{1 - \eta_L^{GPL} V_{GPL}} \right) E_M + \frac{5}{8} \left(\frac{1 + \xi_W^{GPL} \eta_W^{GPL} V_{GPL}}{1 - \eta_W^{GPL} V_{GPL}} \right) E_M \quad (2)$$

so that ξ_L^{GPL} and ξ_W^{GPL} define two geometrical factors indicating the impacts of graphene configuration and scales as (Barati and Zenkour 2018a)

$$\xi_L^{GPL} = \frac{2l_{GPL}}{t_{GPL}} \quad (3a)$$

$$\eta_L^{GPL} = \frac{(E_{GPL}/E_M) - 1}{(E_{GPL}/E_M) + \xi_L^{GPL}} \quad (3b)$$

$$\xi_W^{GPL} = \frac{2w_{GPL}}{t_{GPL}} \quad (3c)$$

$$\eta_W^{GPL} = \frac{(E_{GPL}/E_M) - 1}{(E_{GPL}/E_M) + \xi_W^{GPL}} \quad (3d)$$

so that w_{GPL} , l_{GPL} , and t_{GPL} define platelets average widths, length, and thickness, respectively. Furthermore, Poisson's ratio for graphene based composite might be defined based upon Poisson's ratio of the two constituents in the form

$$\begin{aligned} v_1 &= v_{GPL} V_{GPL} + v_M V_M \\ \alpha_1 &= \alpha_{GPL} V_{GPL} + \alpha_M V_M \end{aligned} \quad (4)$$

in which $V_M = 1 - V_{GPL}$ expresses the volume fractions of matrix component. Herein, three dispersions of the platelets have been assumed as:

Uniform:

$$W_{GPL} = \lambda_1 W_{GPL}^0 \quad (5a)$$

Linear:

$$W_{GPL} = \lambda_2 W_{GPL}^0 \left(\frac{z}{h} + \frac{1}{2} \right) \quad (5b)$$

Nonlinear:

$$W_{GPL} = \frac{\lambda_3 W_{GPL}^0 z^2}{s^2 h^2 (4s^2 - h^2)} \left[4h^2 z^2 - h^4 + \frac{16s^2}{n} (s^2 - z^2) \right], \quad s = 0.45h \quad (5c)$$

where $W_{GPL}^0 = 1\%$ expresses a particular weight fraction for graphene platelets.

With the employment of classical beam theory, a displacement field having following forms might be expressed to start mathematical modeling of the microbeam

$$\mathbf{u}_1(\mathbf{x}, \mathbf{z}) = \mathbf{u}(\mathbf{x}) - \mathbf{z} \frac{\partial \mathbf{w}}{\partial \mathbf{x}} \tag{6a}$$

$$\mathbf{u}_3(\mathbf{x}, \mathbf{z}) = \mathbf{w}(\mathbf{x}) \tag{6b}$$

Here, $u(x)$ and $w(x)$ express the axial and transverse field coefficients. For the classic beam mode, the strain field including geometric imperfection deflection (w^*) might be expressed by (Emam 2009)

$$\begin{aligned} \varepsilon_x &= \frac{\partial u}{\partial x} + \frac{1}{2} \left[\left(\frac{\partial w}{\partial x} \right)^2 - \left(\frac{\partial w^*}{\partial x} \right)^2 \right] - z \left(\frac{\partial^2 w}{\partial x^2} - \frac{\partial^2 w^*}{\partial x^2} \right) \\ \gamma_{xz} &= 0 \end{aligned} \tag{7}$$

Moreover, in order to take into account couple stress effects, there is a need to define the curvature tensor components as

$$\chi_{xy} = -\frac{1}{2} \frac{\partial^2 w}{\partial x^2} \qquad \chi_{xx} = \chi_{yy} = \chi_{zz} = \chi_{xz} = \chi_{yz} = 0 \tag{8}$$

Now, one can express the following constitutive relations based on couple stress coefficient (l) and Lamé's constants (λ_{nc}, μ_{nc}) as (Ebrahimi and Barati 2018)

$$\sigma_{xx} = [\lambda_{nc} + 2\mu_{nc}] \varepsilon_{xx} \tag{9}$$

$$m_{xy} = 2\mu_{nc} l^2 \chi_{xy} \tag{10}$$

So that

$$\lambda_{nc} = \frac{E_1 v_1}{[1 + v_1][1 - 2v_1]} \tag{11}$$

$$\mu_{nc} = \frac{E_1}{2[1 + v_1]} \tag{12}$$

For a microbeam, the governing equations based on classic beam theory and couple stress effects may be expressed by (Emam 2009)

$$\frac{\partial N_x}{\partial x} = 0 \tag{13}$$

$$\frac{\partial^2 M_x^b}{\partial x^2} + \frac{\partial^2 Y_1}{\partial x^2} = -\frac{\partial}{\partial x} \left(N_x \frac{\partial w}{\partial x} \right) + k_L w - k_P \nabla^2 w + k_{NL} w^3 \tag{14}$$

so that k_L , k_P , and k_{NL} define Winkler, Pasternak and nonlinear foundation factors. Then, the resultants in above relations might be written by

$$N_x = A \left[\frac{\partial u}{\partial x} + \frac{1}{2} \left(\frac{\partial w}{\partial x} \right)^2 - \frac{1}{2} \left(\frac{\partial w^*}{\partial x} \right)^2 \right] - B \left(\frac{\partial^2 w}{\partial x^2} - \frac{\partial^2 w^*}{\partial x^2} \right) - N^T \tag{15}$$

$$M_x^b = B \left[\frac{\partial u}{\partial x} + \frac{1}{2} \left(\frac{\partial w}{\partial x} \right)^2 - \frac{1}{2} \left(\frac{\partial w^*}{\partial x} \right)^2 \right] - D \left(\frac{\partial^2 w}{\partial x^2} - \frac{\partial^2 w^*}{\partial x^2} \right) \quad (16)$$

$$Y_1 = -\tilde{A} \left(\frac{\partial^2 w}{\partial x^2} - \frac{\partial^2 w^*}{\partial x^2} \right) \quad (17)$$

where N^T is in-plane thermal loading: $N^T = \int_{-h/2}^{h/2} E_1 \alpha_1 \Delta T dz$ and ΔT is temperature rise.

$$\begin{aligned} A &= \int_{-h/2}^{h/2} \left(\lambda_{nc} \frac{1 - \nu_1}{\nu_1} \right) dz, B = \int_{-h/2}^{h/2} \left(\lambda_{nc} \frac{1 - \nu_1}{\nu_1} \right) z dz, \\ D &= \int_{-h/2}^{h/2} \left(\lambda_{nc} \frac{1 - \nu_1}{\nu_1} \right) z^2 dz, \\ \tilde{A} &= \int_{-h/2}^{h/2} \mu_{nc} l^2 dz, \end{aligned} \quad (18)$$

As final step, obtained governing equations of microbeams having geometrical imperfection according to displacement variables might be written after placing Eqs. (15)-(17) into Eqs. (13) and (14) as

$$A \left(\frac{\partial^2 u}{\partial x^2} \right) - B \left(\frac{\partial^3 w}{\partial x^3} - \frac{\partial^3 w^*}{\partial x^3} \right) + A \left(\frac{\partial w}{\partial x} \frac{\partial^2 w}{\partial x^2} - \frac{\partial w^*}{\partial x} \frac{\partial^2 w^*}{\partial x^2} \right) = 0 \quad (19)$$

$$\begin{aligned} B \frac{\partial}{\partial x} \left(\frac{\partial^2 u}{\partial x^2} + \frac{\partial w}{\partial x} \frac{\partial^2 w}{\partial x^2} - \frac{\partial w^*}{\partial x} \frac{\partial^2 w^*}{\partial x^2} \right) - (D + \tilde{A}) \left(\frac{\partial^4 w}{\partial x^4} - \frac{\partial^4 w^*}{\partial x^4} \right) \\ + \frac{\partial}{\partial x} \left(N_x \frac{\partial w}{\partial x} \right) - k_L (w - w^*) + k_p \nabla^2 (w - w^*) - k_{NL} (w - w^*)^3 = 0 \end{aligned} \quad (20)$$

An important conclusion from Eq. (19) is

$$\frac{\partial}{\partial x} \left(A \frac{\partial u}{\partial x} + \frac{A}{2} \left(\frac{\partial w}{\partial x} \right)^2 - \frac{A}{2} \left(\frac{\partial w^*}{\partial x} \right)^2 - B \left(\frac{\partial^2 w}{\partial x^2} - \frac{\partial^2 w^*}{\partial x^2} \right) \right) = 0 \quad (21)$$

Then, above relation gives

$$\frac{\partial u}{\partial x} = -\frac{1}{2} \left(\frac{\partial w}{\partial x} \right)^2 + \frac{1}{2} \left(\frac{\partial w^*}{\partial x} \right)^2 + \frac{B}{A} \left(\frac{\partial^2 w}{\partial x^2} - \frac{\partial^2 w^*}{\partial x^2} \right) + \frac{c_1}{A} \quad (22)$$

Next, an integration of Eq. (22) results in

$$u = -\frac{1}{2} \int_0^x \left(\frac{\partial w}{\partial x} \right)^2 dx + \frac{1}{2} \int_0^x \left(\frac{\partial w^*}{\partial x} \right)^2 dx + \frac{B}{A} \left(\frac{\partial w}{\partial x} - \frac{\partial w^*}{\partial x} \right) + \frac{c_1}{A} x + c_2 \quad (23)$$

There are two cases of in-plane boundary conditions for the microbeams based on the type of

applied load. When applying a mechanical load (P) the conditions are: $u(0) = 0, u(L) = -PL/A$. When applying thermal loading they are $u(0) = 0, u(L) = 0$. Introducing the boundary conditions for the case of mechanical load leads to

$$\begin{aligned}
 c_2 &= -\frac{B}{A} \left(\frac{\partial w}{\partial x} - \frac{\partial w^*}{\partial x} \right) \Big|_{x=0} = 0 \\
 c_1 &= -P + \frac{A}{2L} \int_0^L \left(\frac{\partial w}{\partial x} \right)^2 dx - \frac{A}{2L} \int_0^L \left(\frac{\partial w^*}{\partial x} \right)^2 dx \\
 &\quad - \frac{B}{L} \left(\frac{\partial w}{\partial x} - \frac{\partial w^*}{\partial x} \right) \Big|_{x=L} + \frac{B}{L} \left(\frac{\partial w}{\partial x} - \frac{\partial w^*}{\partial x} \right) \Big|_{x=0} = 0
 \end{aligned} \tag{24}$$

Based on above constants, Eq. (22) finds the following form

$$\begin{aligned}
 \frac{\partial u}{\partial x} &= -\frac{1}{2} \left(\frac{\partial w}{\partial x} \right)^2 + \frac{1}{2} \left(\frac{\partial w^*}{\partial x} \right)^2 + \frac{B}{A} \left(\frac{\partial^2 w}{\partial x^2} - \frac{\partial^2 w^*}{\partial x^2} \right) - \frac{P}{A} + \frac{1}{2L} \int_0^L \left(\frac{\partial w}{\partial x} \right)^2 dx \\
 &\quad - \frac{1}{2L} \int_0^L \left(\frac{\partial w^*}{\partial x} \right)^2 dx - \frac{B}{LA} \left(\frac{\partial w_b}{\partial x} - \frac{\partial w_b^*}{\partial x} \right) \Big|_{x=L} + \frac{B}{LA} \left(\frac{\partial w_b}{\partial x} - \frac{\partial w_b^*}{\partial x} \right) \Big|_{x=0} = 0
 \end{aligned} \tag{25}$$

Based on above relation, it is possible to derive

$$\frac{\partial^2 u}{\partial x^2} = -\frac{\partial w}{\partial x} \frac{\partial^2 w}{\partial x^2} + \frac{\partial w^*}{\partial x} \frac{\partial^2 w^*}{\partial x^2} + \frac{B}{A} \left(\frac{\partial^3 w}{\partial x^3} - \frac{\partial^3 w^*}{\partial x^3} \right) \tag{26}$$

$$\frac{\partial^3 u}{\partial x^3} = -\left(\frac{\partial^2 w}{\partial x^2} \right)^2 - \frac{\partial w}{\partial x} \frac{\partial^3 w}{\partial x^3} + \left(\frac{\partial^2 w^*}{\partial x^2} \right)^2 + \frac{\partial w^*}{\partial x} \frac{\partial^3 w^*}{\partial x^3} + \frac{B}{A} \left(\frac{\partial^4 w}{\partial x^4} - \frac{\partial^4 w^*}{\partial x^4} \right) \tag{27}$$

The final governing equation for the microbeam will be derived after placing Eqs. (25)-(27) in Eq. (20) as

$$\begin{aligned}
 &\frac{B^2}{A} \left(\frac{\partial^4 w}{\partial x^4} - \frac{\partial^4 w^*}{\partial x^4} \right) + A \left[-\frac{P}{A} + \frac{1}{2L} \int_0^L \left(\frac{\partial w}{\partial x} \right)^2 dx - \frac{1}{2L} \int_0^L \left(\frac{\partial w^*}{\partial x} \right)^2 dx \right. \\
 &\quad \left. - \frac{B}{LA} \left(\frac{\partial w}{\partial x} - \frac{\partial w^*}{\partial x} \right) \Big|_{x=L} + \frac{B}{LA} \left(\frac{\partial w}{\partial x} - \frac{\partial w^*}{\partial x} \right) \Big|_{x=0} \right] \frac{\partial^2 w}{\partial x^2} \\
 &\quad - k_L(w - w^*) + k_p \nabla^2(w - w^*) - k_{NL}(w - w^*)^3 - (D + \tilde{A}) \left(\frac{\partial^4 w}{\partial x^4} - \frac{\partial^4 w^*}{\partial x^4} \right) = 0
 \end{aligned} \tag{28}$$

3. Method of solution

The governing equation for microbeam only contains transverse displacement (w) which needs to be approximated based on following assumption (Ebrahimi and Barati 2017, Hadji *et al.* 2015)

$$w = \sum_{i=1}^{\infty} W_i Q_i(x) \quad (29)$$

So that W_i define the maximum amplitudes and $Q_i(x) = 0.5 \left(1 - \cos\left(\frac{2i\pi}{L}x\right)\right)$ is called shape functions of a clamped-clamped microbeam having below condition

$$w|x=0 = w|x=L = 0, \quad \frac{\partial w}{\partial x}|x=0 = \frac{\partial w}{\partial x}|x=L = 0 \quad (30)$$

Herein, the microbeam is considered to be geometrically imperfect. Also, the imperfection shape is considered as first buckling mode of the microbeam as

$$w^* = W^* \Phi = 0.5W^* \left(1 - \cos\left(2\pi\frac{x}{L}\right)\right) \quad (31)$$

Accordingly, placing Eqs. (29)-(31) in obtained governing equation of the microbeam yields the below nonlinear equation based on maximum amplitude \tilde{W}

$$\tilde{K}\tilde{W} + G^* \tilde{W}^3 + \Gamma\tilde{W}^2 + \Psi W^* = 0 \quad (32)$$

where

$$\begin{aligned} \tilde{K} = & -\left(D + \tilde{A} - \frac{B^2}{A}\right)R_{40} - K_L(R_{00}) + K_P(R_{20}) - (P)R_{20} - \frac{A}{2L}(W^*)^2 \int_0^L (\Phi')^2 dx R_{20} \\ & + \frac{B}{LA} \left(\frac{\partial w^*}{\partial x}|x=L - \frac{\partial w^*}{\partial x}|x=0\right) W^* R_{20} - 3k_{NL}(W^*)^2 \int_0^L \Phi \Phi \varphi_i \varphi_i dx \end{aligned} \quad (33)$$

$$G^* = A\left(\frac{1}{2L}R_{11}R_{20}\right) - K_{NL}(R_{0000}) \quad (34)$$

$$\begin{aligned} \Psi = & \left(D + \tilde{A} + \frac{B^2}{A}\right) \int_0^L \Phi^{(4)} \varphi_i dx + k_L \int_0^L \Phi \varphi_i dx \\ & - k_p \int_0^L \Phi^{(2)} \varphi_i dx + k_{NL}(W^*)^3 \int_0^L \Phi \Phi \Phi \varphi_i dx \end{aligned} \quad (35)$$

$$\Gamma = -\frac{B}{LA} \left(\frac{\partial w}{\partial x}|x=L - \frac{\partial w}{\partial x}|x=0\right) R_{20} + 3k_{nl}(W^*) \int_0^L \Phi \varphi_i \varphi_i dx \quad (36)$$

So that in the case of thermal loading one can delete mechanical load and insert N^T in above relations. Also, other coefficients are

$$\begin{aligned} \{R_{00}, R_{20}, R_{40}, R_{11}\} &= \int_0^L \{\varphi_i \varphi_i, \varphi_i'' \varphi_i, \varphi_i'''' \varphi_i, \varphi_i' \varphi_i'\} dx \\ \{R_{0000}\} &= \int_0^L (\varphi_i)^4 dx \end{aligned} \quad (37)$$

The below dimensionless coefficients are also used for further investigations

$$K_L = k_L \frac{L^4}{D}, \quad K_p = k_p \frac{L^2}{D}, \quad K_{NL} = k_{NL} \frac{L^4}{A} \quad (38)$$

4. Discussion on results

This section is devoted to analyzing mechanical-thermal post-buckling behavior of a micro-size beam reinforced with graphene platelets (GPLs) based on geometric imperfection effects. Graphene platelets have three types of dispersion within the structure including uniform-type, linear-type and nonlinear-type. The micro-size beam is considered to be perfect (ideal) or imperfect. All of material properties have been expressed in Tables 1 and 2. Buckling mode shape of the micro-size beam has been assumed as geometric imperfection. Modified couple stress theory has been used for describing scale-dependent character of the beam having micro dimension. In the following paragraphs, the results are first validated by previous data and then new findings are presented.

Table 1 Gradient index effect on total content of GPLs

Uniform (λ_1)	Linear (λ_2)	Nonlinear (λ_3)	%W* _{GPL}
0	0	0	0
0.33	0.67	0.43	0.33
1	2	1.29	1

Table 2 Material and geometrical parameters for a GPL-reinforced beam

GPLs	Matrix (Epoxy resin)
$E_{GPL} = 1.01$ TPa	$E_M = 2.85$ GPa
$\rho_{GPL} = 1062.5$ kg/m ³	$\rho_M = 1200$ kg/m ³
$\nu_{GPL} = 0.006$	$\nu_M = 0.34$
$\alpha_{GPL} = 2.35 \times 10^{-5}/K$	$\alpha_M = 8.2 \times 10^{-5}/K$
$t_{GPL} = 1.5$ nm	-
$w_{GPL} = 1.5$ μ m	-
$l_{GPL} = 2.5$ μ m	-

Table 3 Verification of nonlinear buckling loads for laminated GPLs reinforced beams ($W_{GPL} = 0.3\%$, $\bar{W}/h=1$)

Number of layers	Yang <i>et al.</i> (2017)	present
4	0.1175	0.1174
6	0.1192	0.1190
10	0.1201	0.1200
28	0.1205	0.1205

First, according to Table 3 nonlinear buckling load of laminated graphene-reinforced beams has been verified with those of Yang *et al.* (2017). For this comparison, different number of layers in laminated composite material are considered and obtained buckling loads are very close to those of Yang *et al.* (2017). So, it may be deduced that presented solution and mathematical model of the graphene reinforced beam in our article is accurate.

Fig. 3 illustrates nonlinear buckling load of graphene based C-C microbeams with respect to normalized amplitude with/without geometry imperfection based upon diverse graphene weight fractions and diffusions. For presenting this figure, other factors are set as $l/h = 0.4$, $L/h = 20$,

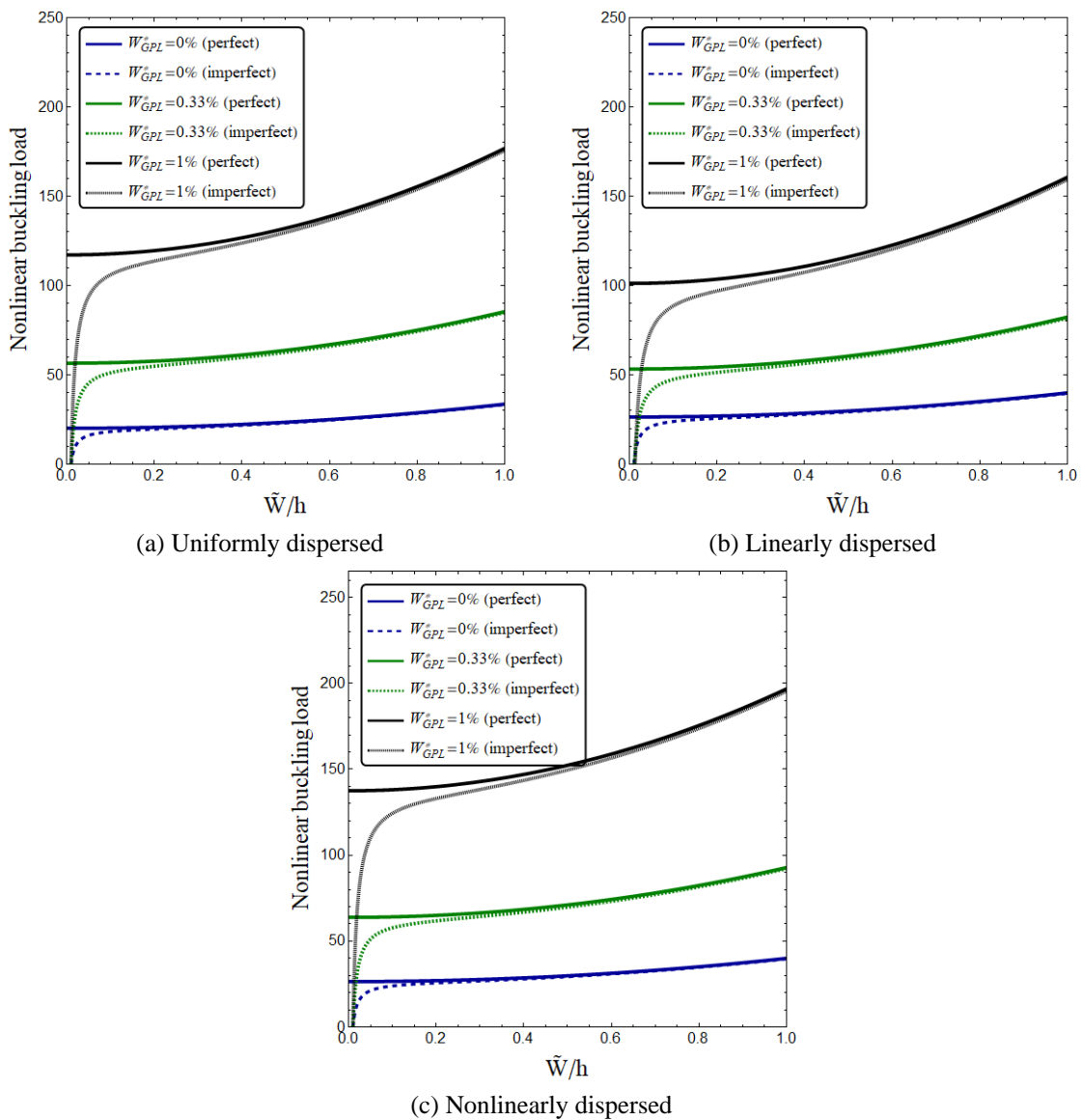


Fig. 3 Impact of graphene weight fraction on nonlinear buckling path of the micro-scale beam ($L/h = 20$, $K_w = 0$, $K_p = 0$, $W^* = 0.01h$, $l/h = 0.4$)

$K_w = 0$, $K_p = 0$ and $W^* = 0.01 h$. In order to obtain critical buckling load of the graphene based microbeam, one may set the normalized amplitude to zero, $\tilde{W}/h = 0$. However, the critical buckling load exists for perfect beams with nonzero value of imperfection amplitude. The main conclusion based on this figure is that increase of graphene weight fraction gives greater nonlinear buckling load owing to rigidity growth of the microbeam. However, the greatest and lowest nonlinear buckling load have been observed based on nonlinear and linear graphene diffusions.

Couple stress impacts on post-buckling curves of ideal and imperfect graphene based microbeams are shown in Fig. 4. For presenting this figure, other factors are set as $L/h = 20$, $K_w = 0$, $K_p = 0$ and $W^* = 0.01 h$. Also, nonlinear graphene dispersion with $W^*_{GPL} = 1\%$ has been selected. At micron scales, two particles apply couple stresses to each other and experience micro rotation. Modified couple stress theory introducing one scale coefficient is able to consider the

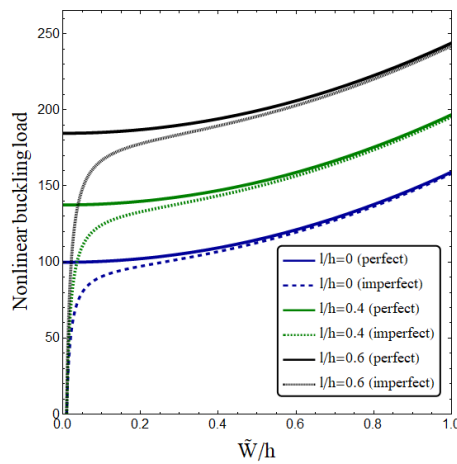


Fig. 4 Impact of couple stress coefficient on nonlinear buckling path of the micro-scale beam ($L/h = 20$, $K_w = 0$, $K_p = 0$, $W^* = 0.01h$, $W^*_{GPL} = 1\%$)

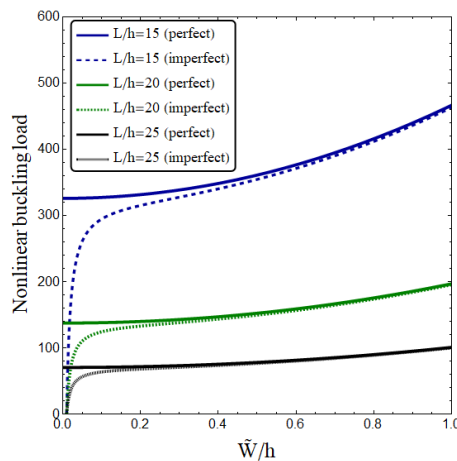


Fig. 5 Impact of slenderness ratio on nonlinear buckling path of the micro-scale beam ($l/h = 0.4$, $W^* = 0.01h$, $W^*_{GPL} = 1\%$)

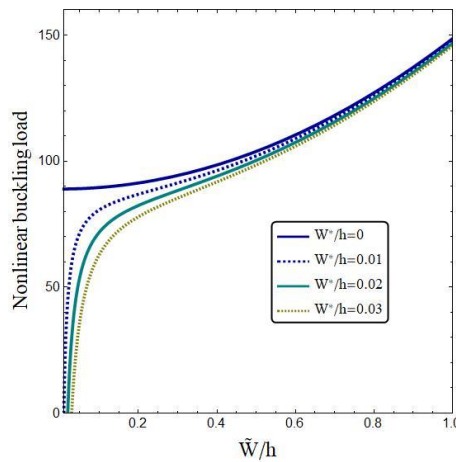


Fig. 6 Impact of imperfection amplitude on nonlinear buckling path of the micro-scale beam ($L/h = 20, l/h = 0.2, W^*_{GPL} = 1\%$)

micro rotation effects. Increase of couple stress coefficient results in greater nonlinear buckling loads owing to rigidity growth of the microbeam.

Fig. 5 indicates the impacts of slenderness ratio (L/h) on nonlinear buckling path of graphene based microbeams. For this figure, nonlinear graphene dispersion with $W^*_{GPL} = 1\%$ has been selected. The microbeams having larger slenderness ratio are less rigid and possess lower buckling load. Therefore, increasing in slenderness ratios will reduce the value of nonlinear buckling loads. Such conclusion can be expressed for either ideal or imperfect microbeams.

Impact of imperfection amplitude on nonlinear buckling path of the micro-scale beam has been shown in Fig. 6. One may observe that the discrepancy among buckling loads according to perfect and imperfect microbeams is negligible at huge normalized amplitude (\tilde{W}/h). Thus, geometrical imperfection impact is more significant at low normalized amplitude.

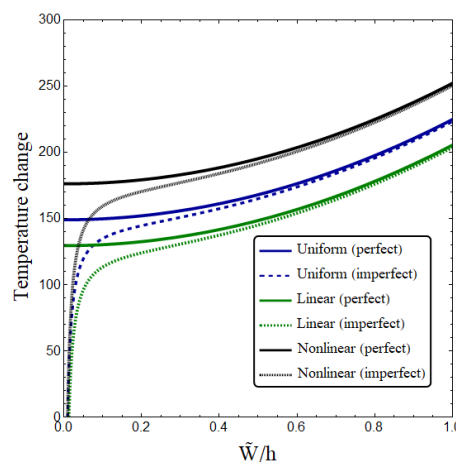


Fig. 7 Impact of graphene distribution on thermal post-buckling path of the micro-scale beam ($L/h = 20, l/h = 0.4, W^*_{GPL} = 1\%$)

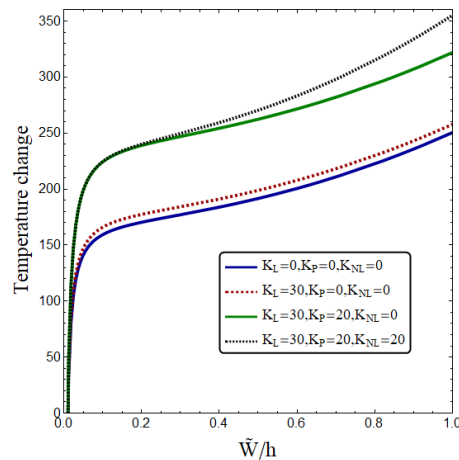


Fig. 8 Impact of foundation factors on thermal post-buckling path of the micro-scale beam ($L/h = 20$, $l/h = 0.4$, $W^*_{GPL} = 1\%$)

Fig. 7 illustrates the impact of graphene distribution on thermal post-buckling path of the micro-scale beam modeled by modified couple stress theory. For presenting this figure, other factors are set as $L/h = 20$, $K_w = 0$, $K_p = 0$ and $W^* = 0.01 h$. The three graphene distribution types with $W^*_{GPL} = 1\%$ are selected. It is clear from the figure that nonlinear graphene distribution is corresponding to highest buckling loads among considered distributions. However, the buckling loads based on uniform graphene distribution are among linear and nonlinear distributions. So, thermal post-buckling of graphene reinforced microbeams are influenced by the graphene distribution type.

Nonlinear post-buckling temperatures versus normalized amplitude according to various foundation factors are plotted in Fig. 8 when $l/h = 0.4$. Nonlinear graphene distribution with $W^*_{GPL} = 1\%$ has been assumed for this graph. All foundation factors result in greater buckling temperatures. It is obvious that nonlinear factor of elastic substrate (K_{NL}) exerts no impact on buckling temperature at smaller amplitude while its impact is more significant at larger amplitude.

5. Conclusions

The presented research examined mechanical-thermal post-buckling of geometrically imperfect microbeams made of graphene based composites. Graphene platelets has three types of dispersion within the structure including uniform-type, linear-type and nonlinear-type. The buckling temperatures or loads were derived based on an analytical procedure. Increase of graphene weight fraction gave greater nonlinear buckling load owing to rigidity growth of the microbeam. However, the greatest and lowest nonlinear buckling load have been observed based on nonlinear and linear graphene diffusions. Increase of couple stress coefficient led to greater nonlinear buckling loads owing to rigidity growth of the microbeam. Also, it was seen that geometrical imperfection impact was more significant at low normalized amplitude.

Acknowledgments

The authors would like to thank Mustansiriyah university (www.uomustansiriyah.edu.iq) Baghdad-Iraq for its support in the present work.

References

- Ahankari, S.S. and Kar, K.K. (2010), "Hysteresis measurements and dynamic mechanical characterization of functionally graded natural rubber-carbon black composites", *Polym. Eng. Sci.*, **50**(5), 871-877. <https://doi.org/10.1002/pen.21601>
- Ahmed, R.A., Fenjan, R.M. and Faleh, N.M. (2019), "Analyzing post-buckling behavior of continuously graded FG nanobeams with geometrical imperfections", *Geomech. Eng., Int. J.*, **17**(2), 175-180. <https://doi.org/10.12989/gae.2019.17.2.175>
- Allahkarami, F. and Nikkhah-Bahrami, M. (2018), "The effects of agglomerated CNTs as reinforcement on the size-dependent vibration of embedded curved microbeams based on modified couple stress theory", *Mech. Adv. Mater. Struct.*, **25**(12), 995-1008. <https://doi.org/10.1080/15376494.2017.1323144>
- Aragh, B.S. (2017), "Mathematical modelling of the stability of carbon nanotube-reinforced panels", *Steel Compos. Struct., Int. J.*, **24**(6), 727-740. <https://doi.org/10.12989/scs.2017.24.6.727>
- Barati, M.R. (2017), "Coupled effects of electrical polarization-strain gradient on vibration behavior of double-layered flexoelectric nanoplates", *Smart Struct. Syst., Int. J.*, **20**(5), 573-581. <https://doi.org/10.12989/sss.2017.20.5.573>
- Barati, M.R. and Zenkour, A.M. (2018a), "Vibration analysis of functionally graded graphene platelet reinforced cylindrical shells with different porosity distributions", *Mech. Adv. Mater. Struct.*, **26**(18), 1580-1588. <https://doi.org/10.1080/15376494.2018.1444235>
- Barati, M.R. and Zenkour, A.M. (2018b), "Analysis of postbuckling behavior of general higher-order functionally graded nanoplates with geometrical imperfection considering porosity distributions", *Mech. Adv. Mater. Struct.*, **26**(12), 1081-1088. <https://doi.org/10.1080/15376494.2018.1430280>
- Barati, M.R. and Zenkour, A.M. (2018c), "Post-buckling analysis of imperfect multi-phase nanocrystalline nanobeams considering nanograins and nanopores surface effects", *Compos. Struct.*, **184**, 497-505. <https://doi.org/10.1016/j.compstruct.2017.10.019>
- Bouafia, K., Kaci, A., Houari, M.S.A., Benzair, A. and Tounsi, A. (2017), "A nonlocal quasi-3D theory for bending and free flexural vibration behaviors of functionally graded nanobeams", *Smart Struct. Syst., Int. J.*, **19**(2), 115-126. <https://doi.org/10.12989/sss.2017.19.2.115>
- Chaudhary, S., Sahu, S.A. and Singhal, A. (2017), "Analytic model for Rayleigh wave propagation in piezoelectric layer overlaid orthotropic substratum", *Acta Mechanica*, **228**(2), 495-529. <https://doi.org/10.1007/s00707-016-1708-0>
- Chaudhary, S., Sahu, S.A., Singhal, A. and Nirwal, S. (2019a), "Interfacial imperfection study in prestressed rotating multiferroic cylindrical tube with wave vibration analytical approach", *Mater. Res. Express*, **6**(10), 105704. <https://doi.org/10.1088/2053-1591/ab3880>
- Chaudhary, S., Sahu, S.A., Dewangan, N. and Singhal, A. (2019b), "Stresses produced due to moving load in a prestressed piezoelectric substrate", *Mech. Adv. Mater. Struct.*, **26**(12), 1028-1041. <https://doi.org/10.1080/15376494.2018.1430265>
- Chaudhary, S., Singhal, A. and Sahu, S.A. (2019c), "Influence of the Imperfect Interface on Love-Type Mechanical Wave in a FGPM Layer", *J. Solid Mech.*, **11**(1), 201-209. <https://doi.org/10.22034/JSM.2019.664229>
- Civalek, Ö. (2017), "Free vibration of carbon nanotubes reinforced (CNTR) and functionally graded shells and plates based on FSDT via discrete singular convolution method", *Compos. Part B: Eng.*, **111**, 45-59. <https://doi.org/10.1016/j.compositesb.2016.11.030>
- Ebrahimi, F. and Barati, M.R. (2017), "Thermal-induced nonlocal vibration characteristics of heterogeneous

- beams”, *Adv. Mater. Res., Int. J.*, **6**(2), 93-128. <https://doi.org/10.12989/amr.2017.6.2.093>
- Ebrahimi, F. and Barati, M.R. (2018), “Stability analysis of porous multi-phase nanocrystalline nonlocal beams based on a general higher-order couple-stress beam model”, *Struct. Eng. Mech., Int. J.*, **65**(4), 465-476. <https://doi.org/10.12989/sem.2018.65.4.465>
- Ebrahimi, F. and Farazmandnia, N. (2017), “Thermo-mechanical vibration analysis of sandwich beams with functionally graded carbon nanotube-reinforced composite face sheets based on a higher-order shear deformation beam theory”, *Mech. Adv. Mater. Struct.*, **24**(10), 820-829. <https://doi.org/10.1080/15376494.2016.1196786>
- Ebrahimi, F. and Habibi, S. (2017), “Low-velocity impact response of laminated FG-CNT reinforced composite plates in thermal environment”, *Adv. Nano Res., Int. J.*, **5**(2), 69-97. <https://doi.org/10.12989/anr.2017.5.2.069>
- Ebrahimi, F. and Habibi, S. (2018), “Nonlinear eccentric low-velocity impact response of a polymer-carbon nanotube-fiber multiscale nanocomposite plate resting on elastic foundations in hygrothermal environments”, *Mech. Adv. Mater. Struct.*, **25**(5), 425-438. <https://doi.org/10.1080/15376494.2017.1285453>
- Ebrahimi, F., Mahmoodi, F. and Barati, M.R. (2017), “Thermo-mechanical vibration analysis of functionally graded micro/nanoscale beams with porosities based on modified couple stress theory”, *Adv. Mater. Res., Int. J.*, **6**(3), 279-301. <https://doi.org/10.12989/amr.2017.6.3.279>
- Emam, S.A. (2009), “A static and dynamic analysis of the postbuckling of geometrically imperfect composite beams”, *Compos. Struct.*, **90**(2), 247-253. <https://doi.org/10.1016/j.compstruct.2009.03.020>
- Esawi, A.M.K., Morsi, K., Sayed, A., Taher, M. and Lanka, S. (2011), “The influence of carbon nanotube (CNT) morphology and diameter on the processing and properties of CNT-reinforced aluminium composites”, *Compos. Part A: Appl. Sci. Manuf.*, **42**(3), 234-243. <https://doi.org/10.1016/j.compositesa.2010.11.008>
- Fantuzzi, N., Tornabene, F., Bacciocchi, M. and Dimitri, R. (2017), “Free vibration analysis of arbitrarily shaped Functionally Graded Carbon Nanotube-reinforced plates”, *Compos. Part B: Eng.*, **115**, 384-408. <https://doi.org/10.1016/j.compositesb.2016.09.021>
- Feng, C., Kitipornchai, S. and Yang, J. (2017), “Nonlinear free vibration of functionally graded polymer composite beams reinforced with graphene nanoplatelets (GPLs)”, *Eng. Struct.*, **140**, 110-119. <https://doi.org/10.1016/j.engstruct.2017.02.052>
- Fenjan, R.M., Ahmed, R.A., Alasadi, A.A. and Faleh, N.M. (2019), “Nonlocal strain gradient thermal vibration analysis of double-coupled metal foam plate system with uniform and non-uniform porosities”, *Coupled Syst. Mech., Int. J.*, **8**(3), 247-257. <https://doi.org/10.12989/csm.2019.8.3.247>
- Gojny, F.H., Wichmann, M.H.G., Köpke, U., Fiedler, B. and Schulte, K. (2004), “Carbon nanotube-reinforced epoxy-composites: enhanced stiffness and fracture toughness at low nanotube content”, *Compos. Sci. Technol.*, **64**(15), 2363-2371. <https://doi.org/10.1016/j.compscitech.2004.04.002>
- Hadji, L., Daouadji, T.H. and Bedia, E.A. (2015), “A refined exponential shear deformation theory for free vibration of FGM beam with porosities”, *Geomech. Eng., Int. J.*, **9**(3), 361-372. <https://doi.org/10.12989/gae.2015.9.3.361>
- Kitipornchai, S., Chen, D. and Yang, J. (2017), “Free vibration and elastic buckling of functionally graded porous beams reinforced by graphene platelets”, *Mater. Des.*, **116**, 656-665. <https://doi.org/10.1016/j.matdes.2016.12.061>
- Lin, F., Yang, C., Zeng, Q.H. and Xiang, Y. (2018), “Morphological and mechanical properties of graphene-reinforced PMMA nanocomposites using a multiscale analysis”, *Computat. Mater. Sci.*, **150**, 107-120. <https://doi.org/10.1016/j.commatsci.2018.03.048>
- Mohammadimehr, M., Monajemi, A.A. and Afshari, H. (2017), “Free and forced vibration analysis of viscoelastic damped FG-CNT reinforced micro composite beams”, *Microsyst. Technol.*, 1-15. <https://doi.org/10.1007/s00542-017-3682-4>
- Mokhtar, Y., Heireche, H., Bousahla, A.A., Houari, M.S.A., Tounsi, A. and Mahmoud, S.R. (2018), “A novel shear deformation theory for buckling analysis of single layer graphene sheet based on nonlocal

- elasticity theory”, *Smart Struct. Systm. Int. J.*, **21**(4), 397-405. <https://doi.org/10.12989/sss.2018.21.4.397>
- Moradi-Dastjerdi, R. and Malek-Mohammadi, H. (2017), “Biaxial buckling analysis of functionally graded nanocomposite sandwich plates reinforced by aggregated carbon nanotube using improved high-order theory”, *J. Sandw. Struct. Mater.*, **19**(6), 736-769. <https://doi.org/10.1177/1099636216643425>
- Mouffoki, A., Bedia, E.A., Houari, M.S.A., Tounsi, A. and Mahmoud, S.R. (2017), “Vibration analysis of nonlocal advanced nanobeams in hygro-thermal environment using a new two-unknown trigonometric shear deformation beam theory”, *Smart Struct. Syst., Int. J.*, **20**(3), 369-383. <https://doi.org/10.12989/sss.2017.20.3.369>
- Nieto, A., Bisht, A., Lahiri, D., Zhang, C. and Agarwal, A. (2017), “Graphene reinforced metal and ceramic matrix composites: a review”, *Int. Mater. Rev.*, **62**(5), 241-302. <https://doi.org/10.1080/09506608.2016.1219481>
- Nirwal, S., Sahu, S.A., Singhal, A. and Baroi, J. (2019), “Analysis of different boundary types on wave velocity in bedded piezo-structure with flexoelectric effect”, *Compos. Part B: Eng.*, **167**, 434-447. <https://doi.org/10.1016/j.compositesb.2019.03.014>
- Park, S.K. and Gao, X.L. (2006), “Bernoulli–Euler beam model based on a modified couple stress theory”, *J. Micromech. Microeng.*, **16**(11), 2355. <https://doi.org/10.1088/0960-1317/16/11/015>
- Reddy, R.M.R., Karunasena, W. and Lokuge, W. (2018), “Free vibration of functionally graded-GPL reinforced composite plates with different boundary conditions”, *Aerosp. Sci. Technol.*, **78**, 147-156. <https://doi.org/10.1016/j.ast.2018.04.019>
- Rostami, R., Mohammadimehr, M., Ghannad, M. and Jalali, A. (2018), “Forced vibration analysis of nano-composite rotating pressurized microbeam reinforced by CNTs based on MCST with temperature-variable material properties”, *Theor. Appl. Mech. Lett.*, **8**(2), 97-108. <https://doi.org/10.1016/j.taml.2018.02.005>
- Sahmani, S and Aghdam, M.M. (2017), “Nonlocal strain gradient beam model for nonlinear vibration of prebuckled and postbuckled multilayer functionally graded GPLRC nanobeams”, *Compos. Struct.*, **179**, 77-88. <https://doi.org/10.1016/j.compstruct.2017.07.064>
- Sahu, S.A., Singhal, A. and Chaudhary, S. (2017), “Influence of Heterogeneity on Rayleigh Wave Propagation in an Incompressible Medium Bonded Between Two Half-Spaces”, *J. Solid Mech.*, 555-567.
- Sahu, S.A., Singhal, A. and Chaudhary, S. (2018), “Surface wave propagation in functionally graded piezoelectric material: an analytical solution”, *J. Intel. Mater. Syst. Struct.*, **29**(3), 423-437. <https://doi.org/10.1177/1045389X17708047>
- Semmah, A., Beg, O.A., Mahmoud, S.R., Heireche, H. and Tounsi, A. (2014), “Thermal buckling properties of zigzag single-walled carbon nanotubes using a refined nonlocal model”, *Adv. Mater. Res., Int. J.*, **3**(2), 77-89. <https://doi.org/10.12989/amr.2014.3.2.077>
- Shenas, A.G., Ziaee, S. and Malekzadeh, P. (2018), “A unified higher-order beam theory for free vibration and buckling of fgcnt-reinforced microbeams embedded in elastic medium based on unifying stress–strain gradient framework”, *Iran. J. Sci. Technol., Transact. Mech. Eng.*, **43**(1), 469-492. <https://doi.org/10.1007/s40997-018-0171-z>
- Singh, M.K., Sahu, S.A., Singhal, A. and Chaudhary, S. (2018), “Approximation of surface wave velocity in smart composite structure using Wentzel–Kramers–Brillouin method”, *J. Intel. Mater. Syst. Struct.*, **29**(18), 3582-3597. <https://doi.org/10.1177/1045389X18786464>
- Singhal, A., Sahu, S.A. and Chaudhary, S. (2018a), “Approximation of surface wave frequency in piezo-composite structure”, *Compos. Part B: Eng.*, **144**, 19-28. <https://doi.org/10.1016/j.compositesb.2018.01.017>
- Singhal, A., Sahu, S.A. and Chaudhary, S. (2018b), “Liouville-Green approximation: An analytical approach to study the elastic waves vibrations in composite structure of piezo material”, *Compos. Struct.*, **184**, 714-727. <https://doi.org/10.1016/j.compstruct.2017.10.031>
- Singhal, A., Sahu, S., Chaudhary, S. and Baroi, J. (2019), “Initial and couple stress influence on the surface waves Transmission in material layers with imperfect interface”, *Mater. Res. Express*, **6**(10), 105713. <https://doi.org/10.1088/2053-1591/ab40e2>
- Wang, X., Yang, H., Song, L., Hu, Y., Xing, W. and Lu, H. (2011), “Morphology, mechanical and thermal properties of graphene-reinforced poly (butylene succinate) nanocomposites”, *Compos. Sci. Technol.*,

- 72(1), 1-6. <https://doi.org/10.1016/j.compscitech.2011.05.007>
- Wu, H.L., Yang, J. and Kitipornchai, S. (2016), "Imperfection sensitivity of postbuckling behaviour of functionally graded carbon nanotube-reinforced composite beams", *Thin-Wall. Struct.*, **108**, 225-233. <https://doi.org/10.1016/j.tws.2016.08.024>
- Yang, J., Wu, H. and Kitipornchai, S. (2017), "Buckling and postbuckling of functionally graded multilayer graphene platelet-reinforced composite beams", *Compos. Struct.*, **161**, 111-118. <https://doi.org/10.1016/j.compstruct.2016.11.048>
- Yazid, M., Heireche, H., Tounsi, A., Bousahla, A.A. and Houari, M.S.A. (2018), "A novel nonlocal refined plate theory for stability response of orthotropic single-layer graphene sheet resting on elastic medium", *Smart Struct. Syst., Int. J.*, **21**(1), 15-25. <https://doi.org/10.12989/sss.2018.21.1.015>
- Zhao, Z., Feng, C., Wang, Y. and Yang, J. (2017), "Bending and vibration analysis of functionally graded trapezoidal nanocomposite plates reinforced with graphene nanoplatelets (GPLs)", *Compos. Struct.*, **180**, 799-808. <https://doi.org/10.1016/j.compstruct.2017.08.044>

CC